Eng. Sci., 2021, **15**, 105–115

Engineered Science

DOI: https://dx.doi.org/10.30919/es8d492

Thermal and Spectral Studies of Transition Metal Complexes of 2-Bromo-3-Hydroxynaphthalene-1,4-Dione: Evaluation of Antibacterial Activity Against Six Bacterial Strains

Umar Ali Dar,[1] Sunita Salunke-Gawali,[1,*] Dnyaneshawar Shinde,[2] Sujit Bhand[1] and Surekha Satpute[3]

Abstract

Synthesis, thermal, spectral, electrochemical, and magnetic properties of transition metal complexes of 2-bromo-3-hydroxynaphthalene-1,4-dione(abbreviated as L) are discussed. The complexes viz, $[Zn(L)_2(H_2O)_2]$; ZnL, $[Cu(L)_2(H_2O)_2]$; CuL, $[Ni(L)_2(H_2O)_2]$; NiL, $[Co(L)_2(H_2O)_2]$; CoL, are resulted from the reactions of L with respective metal chlorides in methanol. The carbonyl frequency (1633 cm^{-1}) of the ligand remains the same in ZnL, whereas it is observed at a higher wavenumber (17 cm^{-1}) in CuL and lower wavenumber (3 cm^{-1}) in NiL and CoL. The thermal decomposition of the complexes was studied by thermogravimetry. Powder X-ray diffraction studies further analyzed the respective metal oxide formed in TG studies. Redox potentials of all complexes are determined by cyclic voltammetry studies. It is difficult to reduce or oxidize the ligand after complexation. The frozen solution (DMSO) spectrum (133 K) of CuL shows four ^{63}Cu hyperfine lines in the $g_{\|}$region with $A_{\|}$ = ~155 G in CuL. The ligand, as well as all-metal complexes, showed considerable antibacterial activity against six strains viz. *Staphylococcus aureus* NCIM (National Collection of Industrial Microorganisms) 2079*, Bacillus subtilis* NCIM 2423*, Escherichia coli* NCIM 2065*, Proteus vulgaris* NCIM 2027*, Pseudomonas aeruginosa* MTCC (Microbial Type Culture Collection and Gene Bank) 2297, *P. putida* MTCC 2463.

Keywords: Lawsone; Thermogravimetric studies; Hydroxynaphthoquinone; Metal complexes; Antibacterial activity.
Received: 18 April 2021; Accepted: 2 July 2021.
Article type: Research article.

1. Introduction

Several transition metal complexes with quinone-based ligands exhibit intramolecular electron transfer between the metal ion and the ligand.[1] Quinones are redox-active molecules that appear in various biological processes, including photosynthesis enzymatic transformations.[2] Quinones can coordinate to the metal ion in three oxidation states viz. (i) quinone, (ii) it's the one-electron reduced form, semiquinone, and (iii) its two-electron reduced form, catechol (Scheme 1). The binding ability of quinone in different oxidation states allows them to play an essential role in biological processes[3,4] Modulation of the reactivity by altering the naphthoquinone's chemical environment attempted to improve their pharmacological activities.[5]

Hydroxynaphthoquinones provide the bidentate or tridentate coordination sites to metal ions; they can also coordinate metal ions in different oxidation states.[6-15] Hydroxynaphthoquinones provide flexible coordination modes for the binding that depend on the experimental conditions; for example, triethylamine can lead to *cis, cis* coordination of ligands, and sodium acetate leads to *trans, trans* coordination of ligand.[16] Heteroleptic complexes can be synthesized with 2,2'-bipyridine and 1,10-phenanthroline.[17] The complexes of hinge-like bis-lawsone complexes showed vapochromic behavior, which could store gases,[18] while others found applications in pharmacology. Iridium complex of 2-hydroxy-1,4-naphthoquinone showed anticancer properties.[19]

Thermogravimetric tools played an important role in deciding the composition of hydroxynaphthoquinones complexes.[6-7] Thermogravimetry can also provide information on the oxidation state of the ligands based on their decomposition. Sometimes these complexes were challenging to crystallize, and there are no single-crystal structures avail-

[1] *Department of Chemistry, Savitribai Phule, Pune University, Pune- 411007, Maharashtra State, India.*
[2] *Department of Chemistry, P.D.E.A's, Prof Ramkrishna More College, Akurdi, Pune 411044, Maharashtra, India.*
[3] *Department of Microbiology, Savitribai Phule Pune University, Pune 411007, Maharashtra, India.*
**E-mail:* sunita.salunke@unipune.ac.in (Sunita Salunke-Gawali)

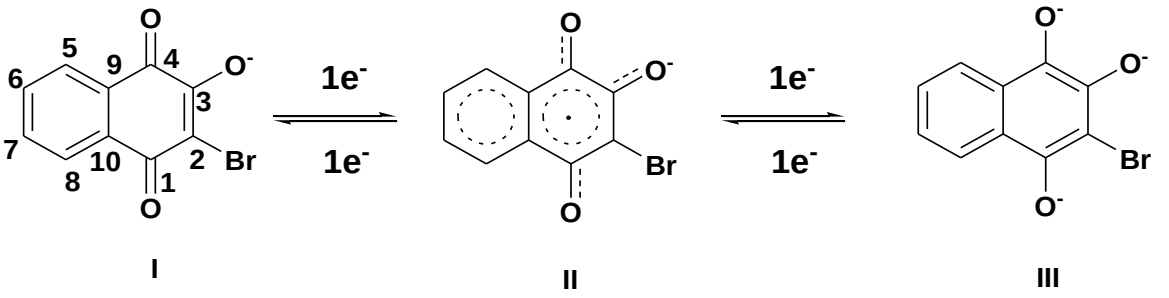

Scheme 1 Various redox forms of ligand L. I (3-bromo-1,4-dioxo-1,4-dihydronaphthalene-2-olate), oxidized form (NQ^-); II (2-bromo-3,4-dihydroxy-1-oxo-1,2-dihydronaphthalene-2-ide), naphthosemiquinone form $(NSQ^-)^-$and III (3-bromonaphthalene-1,2,4-tris(olate)), catechol form (CAT).

able. However, the proposed compositions predicted by thermogravimetry were found precisely the same as those obtained by single-crystal X-ray structures.[8,14-15]

Surprisingly, the coordination chemistry of 2-bromo-3-hydroxynaphthalene-1,4-dione is scarce in literature and has not been relatively exploited, only Fe(II) complex reported by Padhye and coworkers.[20] However, due to applications in the pharmacy and material sciences coordination chemistry of hydroxynaphthoquinone, ligands are fascinating; thus, we report the synthesis, characterizations, thermal, magnetic, and electrochemical behavior in the present work of few first-row transition metal complexes of 2-bromo-3-hydroxynaphthalene-1,4-dione abbreviated as L.

2. Experimental

Chemicals and reagents viz. 2,3-dibromonaphthalene-1,4-dione (DBrNQ) used to synthesize bromolawsone; L, (2-bromo-3-hydroxynaphthalene-1,4-dione) were purchased from Sigma-Aldrich. Methanol, $CuCl_2{\cdot}2H_2O$, $NiCl_2{\cdot}6H_2O$ obtained from Merck Chemicals. $ZnCl_2$, $CoCl_2{\cdot}6H_2O$ were obtained from Qualigen Chemicals and were used without further purification. Anhydrous methanol was prepared according to the procedure mentioned,[21] and Milli-Q water was used to dissolve metal salts.

2.1 Physical Measurements

The products were characterized by various analytical techniques such as (i) Elemental Analysis, (ii) HRMS (High Resolution Mass Spectrometry), (iii) FT-IR (Fourier Transform Infrared Spectroscopy), (iv) UV (Ultraviolet)-Visible, (v) EPR (Electron Paramagnetic Resonance) Spectroscopy, (vi) Room temperature magnetic susceptibility measurements (26 °C), (vii) Atomic Absorption Spectroscopy (AAS), (viii) Thermogravimetric Analysis (TG), (ix) Differential Thermal Analysis (DTA), (x) Differential scanning Calorimetry (DSC), (xi) X-ray powder diffraction studies (PXRD) and (xii) Cyclic voltammetry studies. Elemental analyses are performed on Elementar Vario EL II. Fourier transform infrared spectroscopy (FTIR) spectra of the compounds were recorded between 4000-400 cm^{-1} using KBr pellets on Shimadzu and Bruker Tensor 37 (Fig. S1 through Fig. S4). HRMS spectra recorded on Bruker IMPACT II UHR-TOF (Ultra-High-Resolution Time-Of-Flight) Mass Spectrometer (Fig. S5 through Fig. S8). The UV-Visible spectra of compounds recorded on SHIMADZU UV 1800 in methanol ranging from 200 to 800 nm. The concentration of metal ions was determined by AA-7000 AUTO SAMPLER to Make a SHIMADZU spectrophotometer.

TG-DTA (Thermogravimetry and Differential Thermal Analysis) recorded on SHIMADZU, Model-TA 60 instrument; platinum pan used as the sample holder. The analysis was performed in the air atmosphere.

DSC (Differential Scanning Calorimetry) recorded on SHIMADZU, Make-TA Q2000; Tzero aluminum pan used as sample holder in DSC studies (Fig. S9). X-ray powder diffraction studies (PXRD) were recorded on the RIGAKU Ultima 4 instrument on residues obtained after TG analysis of L metal complexes (Fig. S10). The X-band EPR spectrum of Cu(II) complex was recorded in the solid-state and liquid state at liquid nitrogen temperature (133 K) (Fig. S11)with VARIAN, E112 EPR SPECTROMETER with microwave frequency 9.5 GHz and modulation of frequencies from 100 to 15 Hz at SAIF-IIT Powai, Mumbai, India.

An electrochemical study was performed on CH Instruments electrochemical analyzer (CHI 6054E). IR compensation was done during all the experiments. A conventional three-electrode cell was used to carry out all these experiments. Platinum disc electrode (CHI102, surface area 0.025 cm^2), $Ag/AgNO_3$ (BAS), and platinum wire electrode (CHI115) used as working, reference, and counter electrode, respectively. Before a practical use, the working electrode was polished with 0.05μ alumina powder for one minute, millipore water used for washing, followed by acetone. The actual experiment was done in a fully degassed electrochemical cell, which contains 0.1 M tetra butyl ammonium perchlorate (TEAP) solution of purified anhydrous dimethyl sulphoxide solution (DMSO) with analyte (L, ZnL, CuL, NiL, CoL) concentration 1.3×10^{-3} ML^{-1} for measurements. At the end of the experiments, the potentials were calibrated concerning the normal hydrogen electrode (NHE) using ferrocene as an internal standard. Plots of ip v/s $v^{1/2}$ are presented in Fig. S12 through Fig. S14, and the electrochemical data are presented in Table S2 to Table S4. The magnetic susceptibility experiments were performed on

Faraday balance at room temperature (26 °C) (Table S5 through Table S8).

2.2 Synthesis

2.2.1 Synthesis of 2-bromo-3-hydroxynaphthalene-1,4-dione; L

The ligand L is synthesized according to the literature reported procedure.[25] First, recrystallized 2,3-dibromonaphthalene-1,4-dione 1 g (3.16 mmol) was dissolved in 10 ml of methanol. Next, 20 ml of 2 M KOH was added to this solution with constant stirring at room temperature (26 °C). This mixture was heated for 1 h at 70 °C. As a result, the red-colored precipitate was obtained. This residue was further chilled in the ice bath and dissolved in warm distilled water, followed by neutralization with 2 M HCl. Finally, the yellow-colored precipitate of L was obtained, filtered, and washed with a small amount of methanol and diethyl ether and dried under a vacuum.

2.2.2 Synthesis of metal complexes (ZnL, CuL, NiL, and CoL)

0.2 mmol of ligand L (100 mg) has been dissolved in 15 ml of anhydrous methanol. The solution has been kept stirring for about 30 min at room temperature (26 °C); in this solution, 0.1 mmol of metal salts $ZnCl_2$;(0.027g) (for ZnL), $CuCl_2 \cdot 2H_2O$;(0.033 g) (for CuL), $NiCl_2 \cdot 6H_2O$;(0.046 g) (for NiL), $CoCl_2 \cdot 6H_2O$;(0.047 g) (for CoL), in 2 ml of Milli-Q water was added dropwise with constant magnetic stirring for about 30 min. The colored precipitate was obtained; the reaction mixture was further stirred for 30 min. The precipitate was filtered, and washed with a small amount of methanol and diethyl ether and dried under a vacuum.

2.2.3 Antibacterial activity

Disk diffusion assay was carried out to explore the antibacterial activity of ligand L and its complexes, namely L, CoL, NiL, CuL, and ZnL, against six bacteria, including Gram-positive (02) Gram-negative (04) cultures. In addition to those five compounds, few antibiotics like ampoxin, amoxicillin, ceftriaxone, chloramphenicol, norfloxacin, streptomycin (Himedia Laboratory Pvt. Ltd. India) were included as a reference.[26] The cultures' details are as follows: *Staphylococcus aureus* NCIM (National Collection of Industrial Microorganisms) 2079, *Bacillus subtilis* NCIM 2423, *Escherichia coli* NCIM 2065, *Proteus vulgaris* NCIM 2027, *Pseudomonas aeruginosa* MTCC (Microbial Type Culture Collection and Gene Bank) 2297, *P. putida* MTCC 2463. All cultures were grown and maintained as per the supplier's instructions. Fresh culture inoculums were prepared by inoculating bacteria in a Mueller–Hinton (MH Himedia) medium and incubated overnight at 37 °C. Culture inoculums of the organism to be tested were prepared to equal the turbidity of a 0.5 McFarland standard representing ~1×10^8 colony forming units (CFU) per ml. Around 100 µl of this culture suspension spread on MH agar plates. The wells were punched with the help of a sterile stainless-steel borer, and 30 µl solution of test compounds with varying concentrations viz., 10, 20, 40, 60, 80, and 100 µg/ml added in each well. All compounds dissolved in dimethyl sulfoxide (DMSO), and thus various concentrations were prepared. Antibacterial activity was determined from the zone of inhibition (ZI in cm), and values were reported (Fig. S15). Well filled with DMSO was considered as a negative control.

3. Result and discussion

3.1 Synthesis

In the ligand synthesis, the reaction follows Michael's addition (Scheme 2); the first step in the reaction is fast, *i.e.*, the rate-determining step. Hydroxide anion from KOH acted as a nucleophile and added to C(3) carbon of 2,3-dibromonaphthalene-1,4-dione, resulting in the formation of a salt, *i.e.*, reaction intermediate. The intermediate was dissolved in warm water, followed by a dropwise addition of 2 N HCl. The pH was maintained ~7, which results in the yellow color precipitate, filtered, washed with diethyl ether, dried, and recrystallized from methanol.

The probable reaction mechanism as under for the formation of L is as shown in Scheme 2.

The ligand was synthesized according to the literature reported procedure and characterized by ^1H and ^{13}C NMR (Nuclear Magnetic Resonance), FTIR, elemental analysis, and GC-MS (Gas chromatography-Mass spectroscopy) studies.[25] The procedure used to synthesize the complexes is similar to reported in the literature.[22,25] The synthesis of metal complexes was carried out in dry methanol at room temperature (26 °C) without any catalyst or base. The reaction is supposed to occur by deprotonating the hydroxy group at C(3) position, which coordinates the metal ions, and the L ligand acts as a bidentate ligand[22] The proportion of metal to ligand used was 1:2 in ratio, and the same is observed in metal complexes (Scheme 3). The composition of the complexes was confirmed by elemental analyses (Table 1) and by HRMS.

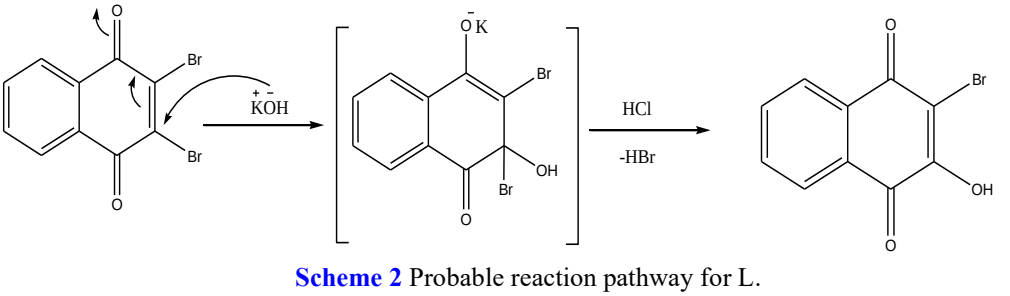

Scheme 2 Probable reaction pathway for L.

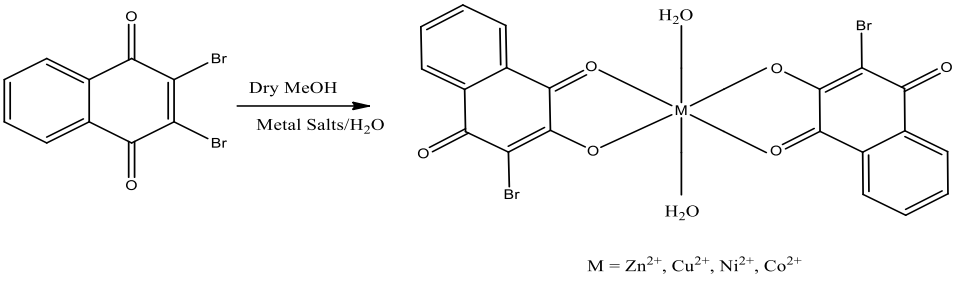

Scheme 3 Reaction scheme for the synthesis of metal complexes.

All the complexes show the mass of $[M(L)_2]Na^+$ type fragments (Fig. S5 through Fig. S8). Metal ion concentration was determined by Atomic Absorption Spectroscopy.

3.2 FTIR studies

The FTIR frequencies observed (Fig. 1) between 3330-3300 cm^{-1} assigned to coordinated $\nu_{(OH)}$ stretching vibrations of a water molecule. After complexation, a shift in frequencies observed for various functional groups is shown in Table 2. The carbonyl stretching frequency for ZnL assigned at 1632 cm^{-1}, which is almost the same as that of the ligand. In CuL, this frequency show shifts to a higher wavenumber (~17 cm^{-1}) at 1650 cm^{-1}. After the deprotonated ligand L, the charge delocalization occurs; moreover, the ligand to metal charge transfer weakens the carbonyl. Thus, there is a decrease in carbonyl frequency observed in IR. For naphthoquinone complexes, the vibrational frequencies of carbonyl are also susceptible to ligand oxidation state. The complexes NiL and

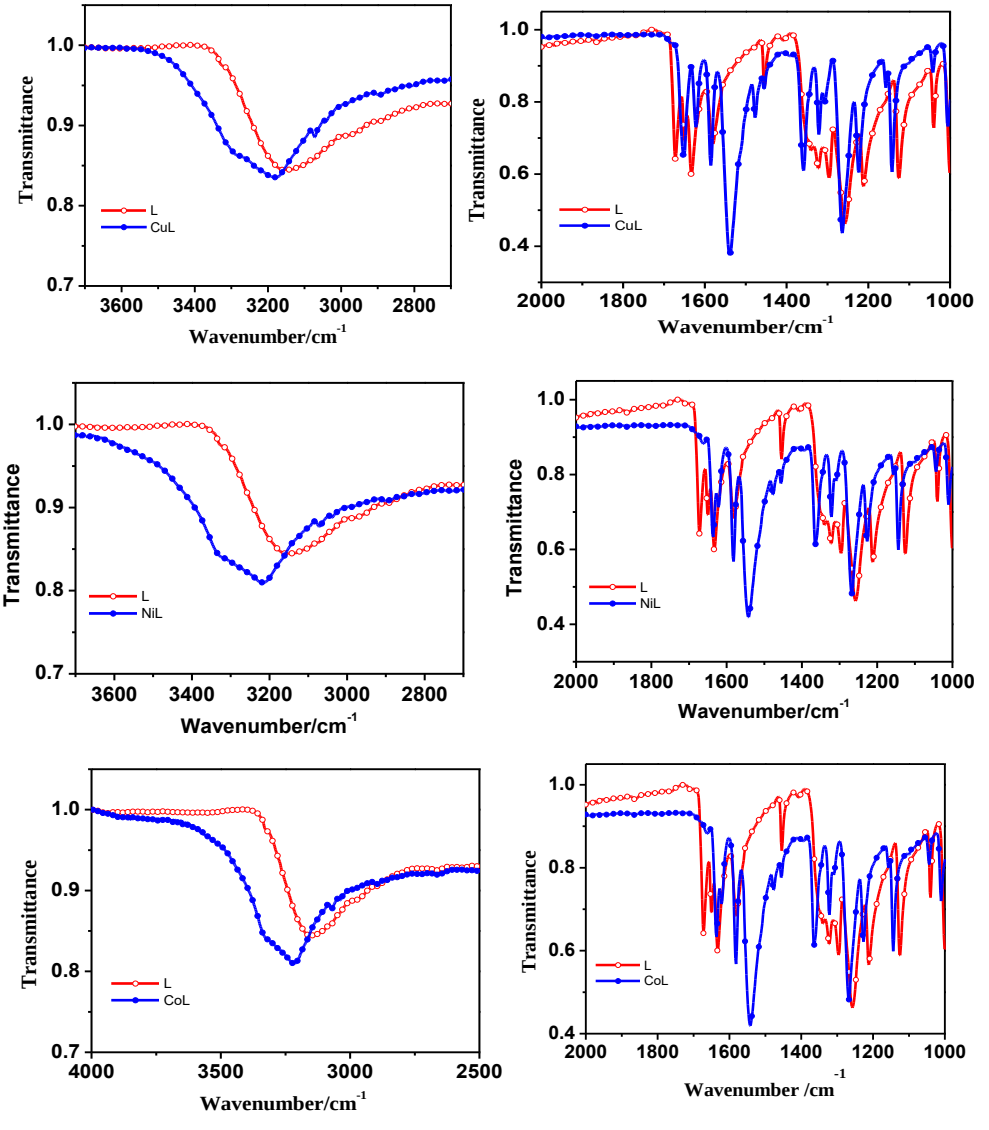

Fig. 1 FTIR spectra of CuL, NiL, CoL.

Table 1. Elemental Analysis and UV-Visible data of L complexes.

Compound	UV-Visible bands	Yield/ %	Composition	Elemental analysis found/Calc./%.			
				M. wt./g	C%	H%	M%
ZnL*	228, 293, 330, 484	81.8	$C_{20}H_{12}Br_2O_8Zn$	605.49	39.52/39.67**	2.14/1.99	10.37 /10.80
CuL	287, 291, 330, 484	74.7	$C_{20}H_{12}Br_2CuO_8$	603.66	39.87/39.79	2.16/2.00	10.36/10.53
NiL	292, 294, 332, 482	42.5	$C_{20}H_{12}Br_2NiO_8$	598.81	40.07/40.12	2.17/2.02	9.91/9.80
CoL	289, 293, 330, 484	95.0	$C_{20}H_{12}Br_2CoO_8$	599.05	40.15/40.09	2.26/2.01	9.76/9.83

* Composition of all complexes are $[M(L)_2(H_2O)_2]$

** Calculated values

Table 2. Significant FT-IR frequencies (/cm^{-1}) of Zn(II), Cu(II), Ni(II), Co(II)complexes of L.

Assignment	$\nu_{(OH)}$	$\nu_{(C-H)}$	$\nu_{(C=O)}$	$\nu_{(C=C)}$	$\nu_{(p-NQ)}$	$\nu_{(C-Br)}$
L	3328		1671, 1633,1583	1585	1222	717, 715
ZnL*	3326	3071	1632	1543	1227	725,727
CuL	3178	3072	1650	1539	1265	723,725
NiL	3302	3071	1629	1542	1271	733
CoL	3217	3072	1629	1541	1269	725,727

*Ref [25]

CoL showed the same stretching frequency of carbonyl at 1629 cm^{-1}. The band from 1543-1535 cm^{-1} in all the complexes was assigned to $\nu_{C=C}$, and ν_{p-NQ} was assigned to frequencies at 1227-1271 cm^{-1}. The C-X bond frequency was assigned from 717-737 cm^{-1} for all the complexes.[23]

3.3 Electronic spectral studies

Electronic spectra (UV-Visible) of all metal complexes are shown in Fig. 2. The spectra are recorded in methanol with a concentration of 1×10^{-4} M. Three transitions bands are observed to all metal complexes; the band at ~286-292 nm and 334-339 nm were assigned to π-π* transitions of naphthoquinone ring, single broadband in the visible region was assigned to n-π* charge transfer (CT) transition.[23]

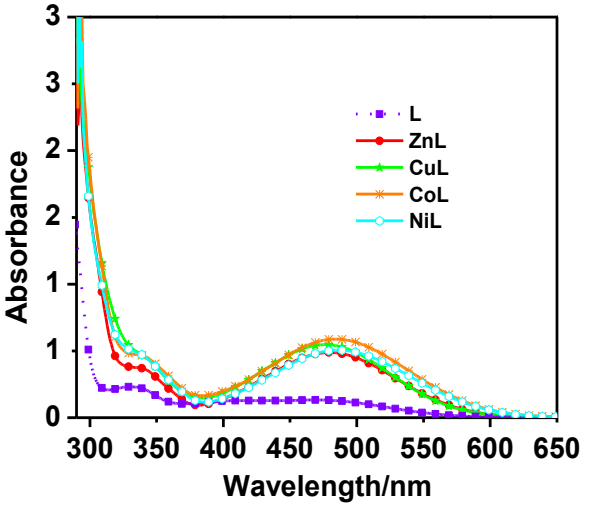

Fig. 2 Electronic spectra of metal complexes of L.

3.4 Thermogravimetric (TG) studies of metal complexes

The thermal study of ligand L was carried out using thermogravimetric analysis (TG), DTA, and DSC studies. Thermogram (TG) of ligand L and its metal complexes are represented in Fig. 3 and are recorded at laboratory constructed instruments[11,13-15] in the range of room temperature 20 °C to 900 °C as well as on Shimadzu TA-60 under air atmosphere at the heating rate is kept as 5 °C / min. Whereas in DSC (Fig. S9), the first small exothermic peak at 171 °C of L suggesting a possible structural phase transition, and the second sharp one at 200 °C corresponds to the melting point of the ligand.

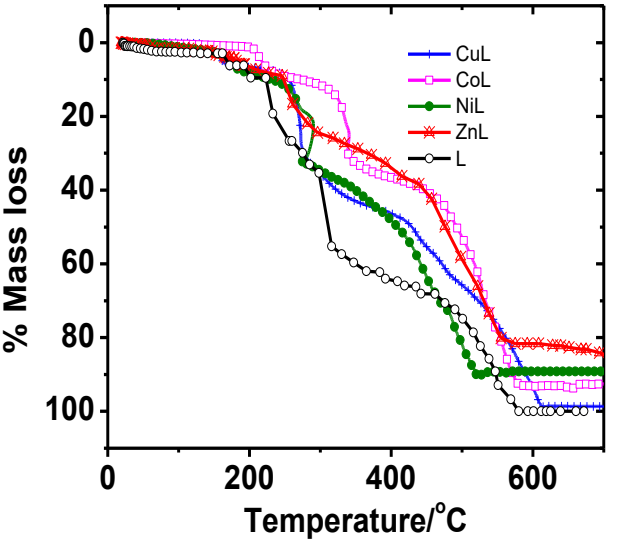

Fig. 3 Thermograms of complexes L and its complexes.

A similar decomposition pattern is observed for the ligand and metal complexes, as shown in Fig. 3. The thermograms revealed that the metal complexes are thermally more stable than the ligand L. Among all complexes, CoL is thermally more stable than other metal complexes. The decomposition of metal complexes takes place clearly in two steps. The first

step involves the loss of axial water ligands, and in step II, abruptly followed by gradual mass loss corresponds to the decomposition of the ligands.

A gradual mass loss starts at ~50 °C for all complexes except for CuL; in CuL, the two water molecules lost in temperature 120 °C -175 °C, with a mass loss of 6.49% (6.04% calculated). The decomposition of water molecules in NiL and ZnL takes place at ~210 °C. CoL being thermally more stable than other complexes, its water molecules were lost at ~200 °C – 243 °C.

As revealed from the single-crystal X-ray diffraction studies, depending on the condition used in the synthesis, hydroxynaphthoquinone-metal complexes exist as *cis, cis*, or *trans, trans* geometry.[24] The complexes synthesized in this investigation possess the *trans*, *trans* geometry of ligands and water molecules. Moreover, these complexes exist as a polymeric network formed by intermolecular O-H··O hydrogen bonding (Fig. 4). The gradual mass loss (1-2%) below 100 °C in the thermogram of ZnL, NiL, and CoL accounts for breaking intermolecular hydrogen bonding (Fig. 4). Early gradual mass loss in TG studies, also supported by DTA (Fig. 5) and DSC studies (Fig. S9), a gradual endotherm is observed.

Abrupt mass loss observed in TG studies at 234 °C, 245 °C, 257 °C, and 285 °C respectively for NiL, ZnL, CuL, and CoL; a phase transition from solid to liquid may occur due to melting of complexes. Abrupt mass loss is ~ 25% -30% over a temperature range of 40 °C, from the respective melting temperature. Sharp exotherms observed in DTA curves (Fig. 5) in the metal complexes' respective temperature range support the phase transition. Further gradual mass loss was noted for all complexes till the end of the decomposition. 100% mass loss was observed for the ligand L as an organic compound ~600 °C. The complete disintegration of all ligands takes place at 520 °C in NiL. In contrast, in CuL, it is at 613 °C with a total mass loss of ~98%, similar to the vapochromic behavior of bis –lawsone complexes of other metals.[18] Respective metal oxides formed at the end of pyrolytic decomposition confirmed from powder XRD.

3.5 X-ray powder diffraction studies

X-ray powder diffraction studies (PXRD) were performed on residues remaining after the complete decomposition of complexes by TG studies up to 700 °C on the laboratory build instrument. The powder diffraction patterns of ZnL, CuL, and NiL complexes are shown in Fig. S10. PXRD data is represented in (Table S1). The presence of respective metal oxide ZnO, CuO, NiO, and CoO formed after thermal decomposition of ZnL, CuL, NiL, and CoL complexes was confirmed by powder X-ray diffraction studies. The mixed crystalline phase of metal oxide is observed in the residues. The θ values of oxides were compared with CCDC data, file numbers 05-0644, 05-0661, 04-0835, and 09-0402.

3.6 Electrochemical studies

Electrochemical investigation of the ligand L and its transition metal complexes was carried out by cyclic voltammetry in the DMSO solution using $Ag/AgNO_3$ reference electrode. All the potentials were corrected against Vs. NHE electrode. The cyclic voltammogram at various scan rates is shown in (Fig. 6), and the corresponding data are presented in (Table S2 to S4). The ligand-based cathodic and anodic peak potential of L to its metal complexes is given below (Table 3).

Several reduction peaks are observed in cyclic voltammogram of CuL, an intense reversible metal-based redox couple is observed at $E_{1/2}$= 0.36V assigned to Cu(II)/Cu(0) redox couple with ΔEp = 0.12 V.[22] The peak at ~ 0.378 V was assigned to Cu(0)/Cu(I).[27] Increases in current were observed with time due to the deposition of copper on the electrode.[27]

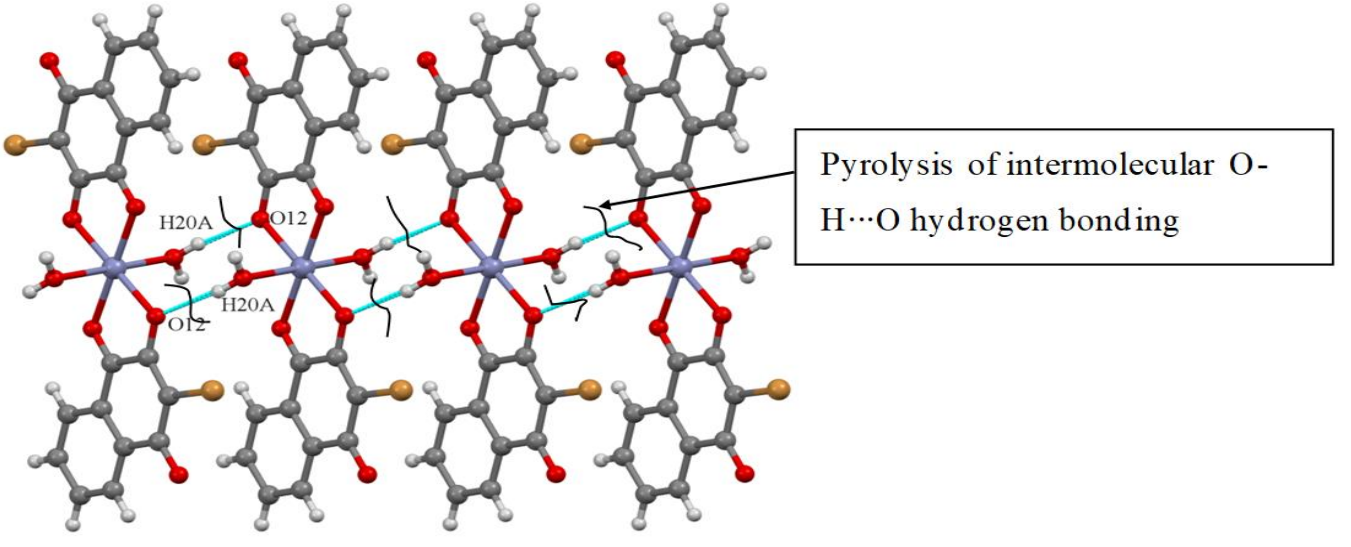

Fig. 4 Polymer chain of $[Zn(L)_2(H_2O)_2]$ formed by O-H···O hydrogen bonding.

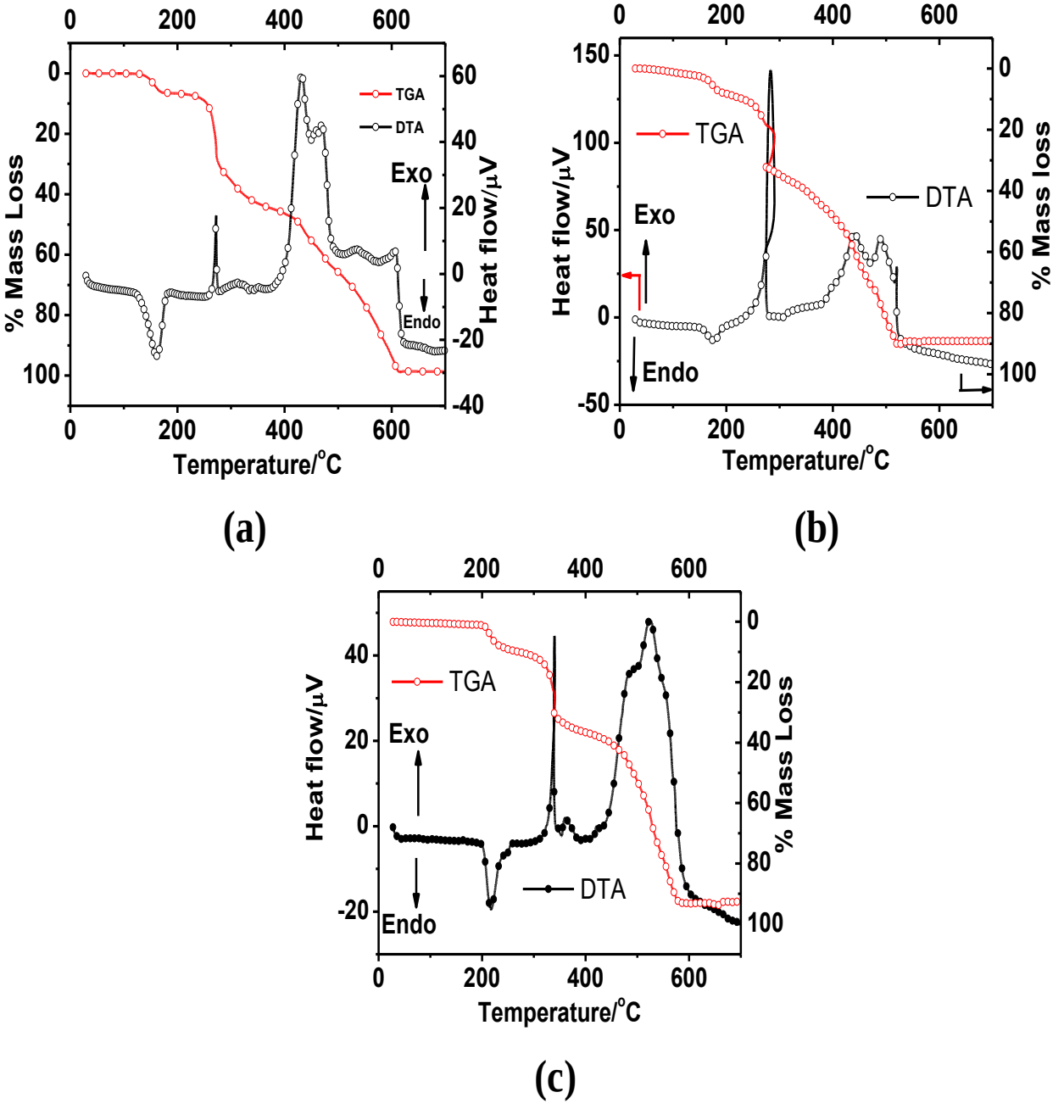

Fig. 5 TG and DTA curves of (a) CuL, (b) NiL, and (c) CoL.

Table 3. Cathodic and anodic peak potentials of ligand L and its complexes at 100 mV.

	Potential/V			
Particulars	Epc(Ic)	Epc(Ia)	Epc(IIc)	Epc(IIa)
L	-0.212	-0.092	-0.954	-0.713
ZnL*	-0.548	-0.477	-1.080	-0.929
CuL	0.298	0.424	0.378	-0.2248
NiL	-0.372	-0.296	-0.538	-0.4545
CoL	-0.421	-0.310	-0.900	-0.758

*Ref [25]

Cyclic voltammogram of NiL shows ligand-based one reversible $E_{1/2}$ = -0.67 V with ΔEp = 0.075 V, and irreversible peaks ΔEp = 0.084 V were observed. The reversible cathodic peak was observed at -0.372 V with a corresponding oxidation peak at -0.296 V, having ΔEp as 75 mV, and an irreversible cathodic peak at -0.538 V; these peaks are associated with the reduction of the ligand.[27]

Two irreversible ligand-based cathodic peaks (-0.903V and 0.4212 V), and two anodic peaks -0.310 V, -0.758V, are observed in cyclic voltammogram of CoL. Possible redox reactions are summarized in (Scheme 4).

3.7 Room temperature magnetic susceptibility studies

Magnetic susceptibility studies of CuL, NiL, and CoL complexes are performed at room temperature (26 °C) using

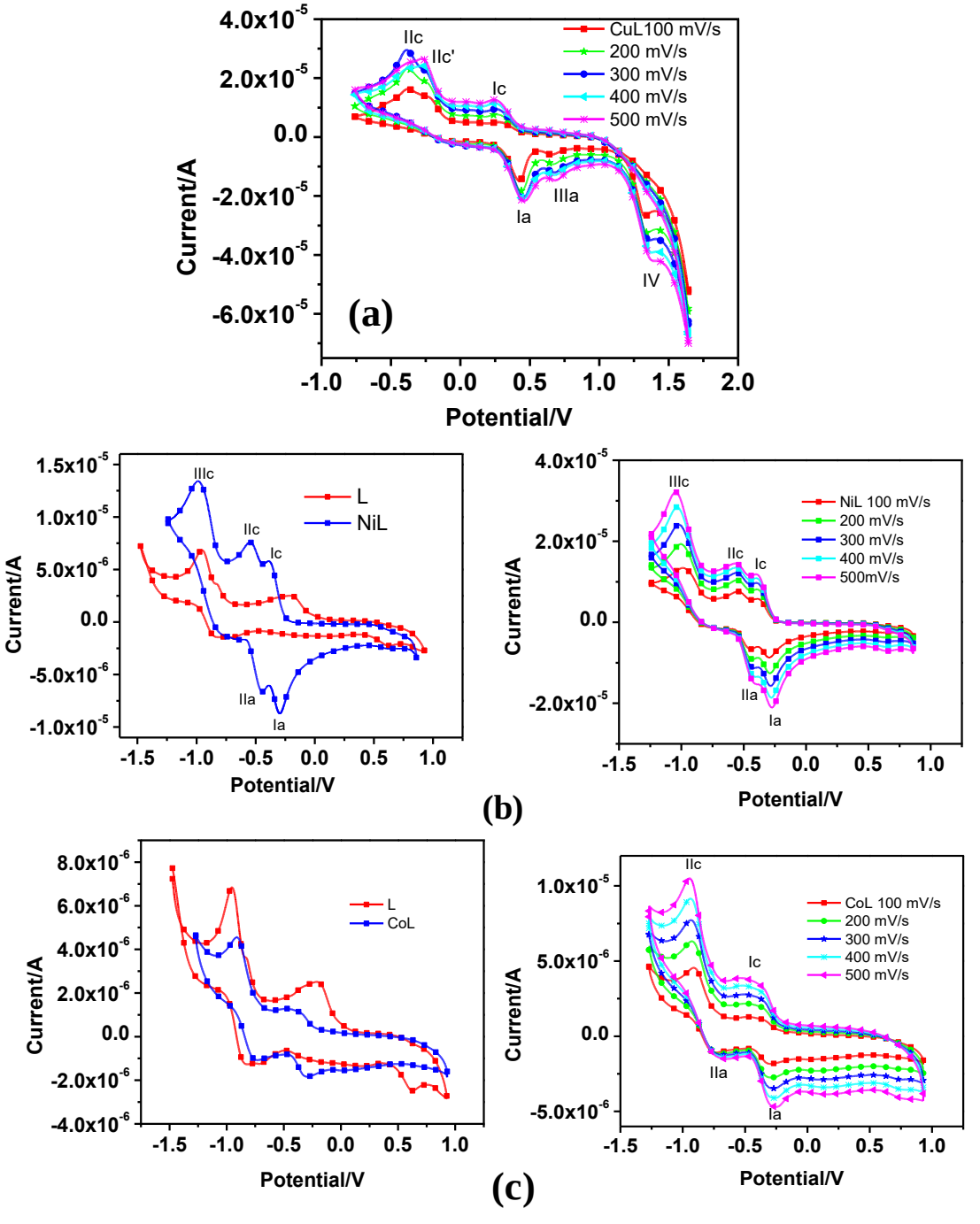

Fig. 6 Cyclic voltammogram of (a) CuL, (b) NiL and (c) CoL, at 100 mV /s (left) and at various scan rates (right).

the Faraday method. The calculated $\mu_{B.M.}$ values are presented in Table 4 (details in Table S5 to Table S8), which agree with octahedral coordination complexes. The magnetic moment of first-row transition elements mainly corresponds due to spin-only values.[28]

3.8 X-band EPR spectroscopy

X-band EPR spectra of the CuL recorded in polycrystalline powder form and DMSO frozen solution at liquid is presented in Fig. 7, Fig. S11, respectively. X-band EPR of Cu(II) complex typically of axial symmetry[29] with $g_{\parallel}$= 2.3570 and $g_{\perp}$ = 2.0784, (Table 5) since $g_{\parallel}>g_{\perp}$, the unpaired electron is

Table 4. Room temperature (26 °C) magnetic susceptibility data for metal complexes.

Particulars	CoL	NiL	CuL
χ_g (cm^3/g)	1.0958 ×10^{-5}	4.491×10^{-6}	1.9626 ×10^{-6}
χ_d (cm^3/mol)	-2.873×10^{-4}	-2.853 ×10^{-4}	-2.8818×10^{-4}
χ_M (cm^3/mol)	6.5672×10^{-3}	2.9745×10^{-3}	1.4729×10^{-3}
$\mu_{B.M.}$ observed	3.96	2.66	1.87
$\mu_{B.M.(spin\ only)}$	3.87	2.83	1.73
Ground Term symbol	^{4}F	^{3}F	^{2}D

residing in the $d_{x^2-y^2}$ orbital of Cu(II).[30-31] The frozen solution (DMSO) spectrum (133 K) showed four hyperfine lines ^{63}Cu in the $g_{\parallel}$ region with $A_{\parallel}$ =~155 G, which is typically observed for monomeric Cu(II).[32] However, any half field signal is absent in polycrystalline powder or solution spectra at 133 K.

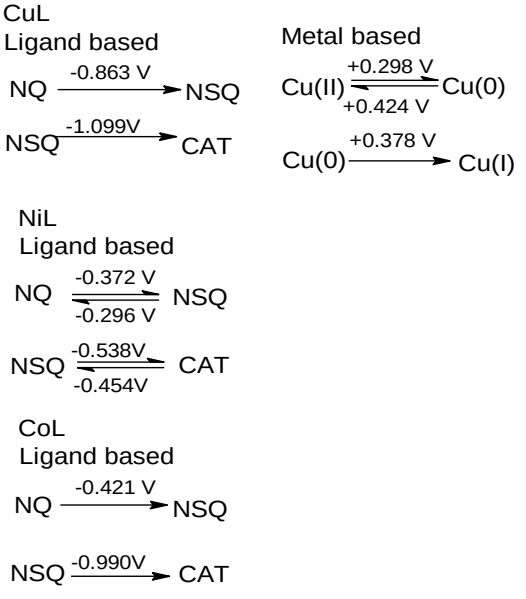

Scheme 4 Probable redox reactions of metal complexes of L.

Table 5. EPR data of CuL complex.

Particulars		$g_{\parallel}$	$g_{\perp}$	$A_{\parallel}$
CuL	Polycrystalline powder	2.357 (2760 G)	2.078 (3130 G)	
	Frozen DMSO solution	2.344 (2775 G)	2.081 (3125 G)	155G

g = 'g'factor
A = hyperfine coupling constant

3.9 Antibacterial activity

It was revealed that the ligand L and its four metal complexes showed considerable antibacterial activity against six strains used in the current investigation. The ZI (zone of inhibition) was found between 0.7 and 1.6 cm at different concentrations of compounds for the ligand and the metal complexes. Results also illustrated a concentration-dependent toxic effect of the complexes. The fact was evident from the ZI, which increased with the increased concentration of the complexes. It is also important to note that, among all complexes, CuL found to be most effective against both Gram-positive bacteria even at a lower concentration (10 to 20 µg/ml). Thus, the best activity of CuL was seen against *S. aureus* NCIM 2079 and *B. subtilis* MTCC 2423 with a ZI of 0.9 cm (at 10 µg/ml) and 1.0 cm (at 20 µg/ml), respectively. This significant increase in the activity of CuL was observed at higher concentrations. For both Gram-positive strains - *S. aureus* NCIM 2079 and *B. subtilis* MTCC 2423, the ZI was found to up to 1.6 cm at a concentration of 100 µg/ml. However, the compound CuL found to be less effective against Gram-negative bacteria at lower concentrations. Except for *E. coli* NCIM 2065, the ZI of CuL was observed to be 0.6 to 0.8 cm at higher concentrations (60, 80, 100 µg/ml) against three Gram-negative bacteria. The compound CuL showed a ZI of 1.0 cm at 100 µg/ml against *E. coli* NCIM 2065. The ligand L exhibited a ZI of 0.8 cm against *E. coli* NCIM 2065 at a concentration of 100 µg/ml. Like CuL, other complexes, CoL was also effective with a ZI of 0.8 cm at a 20 µg/mL concentration against *S. aureus* NCIM 2079. Antibacterial activity of CoL was higher at 100 g/ml with a ZI of 1.3 and 1.2 cm, respectively, for *S. aureus* NCIM 2079. All compounds exhibited a ZI of 0.7 to 0.9 cm against *P. putida* 2463 and *P. vulgaris* NCIM 2027. Moreover, the ligand L and its complex CuL showed an inhibitory effect on *S. aureus* NCIM 2079, *P. putida* MTCC 2463, and *P. vulgaris* NCIM2027, a ZI of 0.7 mm at 100 µg/ml. Two strains, namely *E. coli* NCIM 2065 and *P. aeruginosa* MTCC 2297, were resistant to CoL and NiL even at higher concentrations. The MIC values for all those reference antibiotics were found to be in the range of 2 to 1024 µg/ml. Except for streptomycin

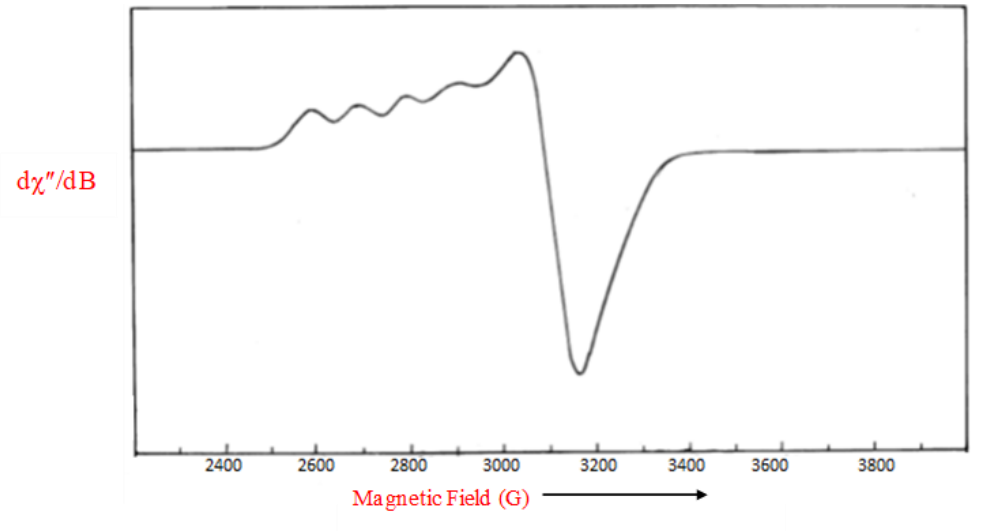

Fig. 7 X-band EPR spectra of CuL in DMSO at 133 K Field Set: 3000G, Scan Range: 2000G, Modulation Amplitude: 1G, Modulation Frequency: 100 kHz, Receiver Gain: $6\times10^2\times10$, Microwave Power: 5mW, Microwave frequency: 9.1GHz.

(16 µg/ml), the MIC of all antibiotics was found to be lowest (2 µg/ml) against *S. aureus*. Relatively high MIC values (4 to 1024 µg/ml) were observed for both *Pseudomonas* strains. Whereas against *B. subtilis* NCIM 2027 and *P. vulgaris* NCIM 2027, MIC was found in the range of 2 to 256 µg/ml. Overall, the antibacterial activities of the test compounds were compared with the reference antibiotics.

4. Conclusions

Cu(II), Ni(II), Co(II)) complexes of ligand 2-bromo-3-hydroxynaphthalene-1,4-dione are synthesized for the first time in this investigation. The composition of the complexes confirmed by thermogravimetric analysis and is of $[M(L)_2(H_2O)_2]$ type. In all complexes, the coordination of ligand and water molecules are *trans*, *trans* to one another. Cyclic voltammetry studies studied the redox nature of the complexes. It isn't easy to reduce the ligand after complex formation with metal ions as the redox potential appeared at higher potentials. Magnetic properties of paramagnetic complexes were studied by room temperature magnetic susceptibility studies and EPR studies (for CuL). The antibacterial potential of the complexes was evaluated against Gram-positive and Gram-negative bacteria. All the complexes showed antibacterial activity.

Acknowledgments

SSG and SS grateful to the Science and Engineering Research Board, Department of Science and Technology, Government of India (Ref. No. EMR/2016/007912) for financial support.

Supporting information

FTIR figures; Fig. S1 through Fig. S4, DSC curves; Fig. 5 through Fig. 8 HRMS; Fig. S9, DSC curves; Fig. S10 PXRD; Fig. S11, EPR spectrum; Cyclic Voltammetry Figures; Fig. S12 through Fig. S14, Fig. S15, Antibacterial activity photograph; Table S1, Electrochemical data; Table S2 through Table S4, Magnetic susceptibility data; Table S5 through Table S8.

Conflict of interest

There are no conflicts to declare.

References

[1] C. G. Pierpont, *Coordin. Chem. Rev.*, 2001, **219-221**, 415-433, doi: 10.1016/S0010-8545(01)00342-3.

[2] A. V. Pinto, S. L. Castro, *Molecules*, 2009, **14**, 4570-4590, doi: 10.3390/molecules14114570.

[3] J. P. Klinman, *Biochem. Biophys. Acta*, 2003, **1647**, 131-137, doi: 10.1016/s1570-9639(03)00077-3.

[4] W. Kaim, *Dalton Trans.*, 2003, 761-68, doi: 10.1039/B210193A.

[5] Z. F. Chen, M. X. Tan, Y. C. Liu, Peng Y, H. H. Wang, H. G. Liu, H. Liang, *J. Inorg. Biochem.*, 2011, **105**, 426-432, doi: 10.1016/j.jinorgbio.2010.12.003.

[6] S. Y. Rane, S. D. Gawali, S. B. Padhye, A. S. Kumbhar, P. P. Bakare, *J. Therm. Anal. Calorim.*, 1999, **55**, 249-258, doi: 10.1023/A:1010121214059.

[7] S. Salunke-Gawali, S. Y. Rane, K. Boukheddaden, E. Codjovi, J. Linares, F. Varret and P. P. Bakare, *Ind. J. Chem.*, 2004, **43A**, 2563-2567.

[8] L. Kathawate, S. P. Gejji, S. D. Yeole, P. L. Verma, V. G. Puranik, S. Salunke-Gawali, *J. Mol. Struc.*, 2015, **1088**, 56-63, doi: 10.1016/j.molstruc.2015.01.053.

[9] S. Y. Rane, S. D. Gawali, S. B. Padhye, A. S. Kumbhar, V. G. Puranik, P. P. Bakare, K. Date, *Proc. Ind. Acad. Sci (ChemSci).*, 1996, **108**, 289.

[10] S. Gawali, R. Dalvi, K. Ahmed and S. Rane, *J. Therm. Anal. Calorim.*, 2004, **76**, 801-812, doi: 10.1023/B:JTAN.0000032265.45347.3d.

[11] S. Salunke-Gawali, S. Y. Rane, K. Boukheddaden, E. Codjovi, J. Linares, F. Varret, P. P. Bakare, *J. Therm. Anal. Calorim.*, 2005, **79**, 669-675, doi: 10.1007/s10973-005-0594-9.

[12] S. Salunke-Gawali, L. Kathawate, Y. Shinde and V. G. Puranik, T. Weyhermüller, *J. Mol. Struc.*, 2012, **1010**, 38-45, doi: 10.1016/j.molstruc.2011.11.015.

[13] L. Kathawate, Y. Shinde, R. Yadav, S. Salunke-Gawali, *J. Therm. Anal. Calorim.*, 2013, **111**, 1003–1011, doi: 10.1007/s10973-012-2378-3.

[14] L. Kathawate, Y. Shinde, R. Yadav, U. Kasabe, M. Nikalje, S. Salunke- Gawali, *J. Therm. Anal. Calorim.*, 2014, **115**, 2319–2330, doi: 10.1007/s10973-013-3204-2.

[15] L. Kathawate, R. Patil, R. Yadav, S. Salunke- Gawali, *J. Therm. Anal. Calorim.*, 2015, **121**, 1185–1195, doi: 10.1007/s10973-015-4575-3.

[16] F. Bustamante, M.M.P. Silva, W. A. Alves, C. B. Pinheiro, J.A.L.C. Resende, M. Lanznaster, *Polyhedron*, 2012, **42**, 43-49, doi: 10.1016/j.poly.2012.04.027.

[17] M. A. Ribeiro, M. Lanznaster, M.M.P. Silva, J.A.L.C. Resende, M.V.B. Pinheiro, K. Krambrock, H. O. Stumpf, C. B. Pinheiro, *Dalton Trans.*, 2013, **42**, 5462-5470, doi: 10.1039/C3DT32968B.

[18] K. Yamada, S. Yagishita, H. Tanaka, K. Tohyama, K. Adachi, S. Kaizaki, H. Kumagai, K. Inoue, R. Kitaura, H. Chang, S. Kitagawa, S. Kawata, *Chem. Eur. J.*, 2004, **10**, 2647-2660, doi: 10.1002/chem.200305640.

[19] S. Oramas-Royo, C. Torrejón, I. Cuadrado, R. Hernández-Molina, S. Hortelano, A. Estévez-Braun, B. Heras, *Bioorg. Med. Chem.*, 2013, **21**, 2471–2477, doi: 10.1016/j.bmc.2013 .03.002.

[20] S. Padhye, P. Garge, M. P. Gupta, *Inorg. Chim. Acta*, 1988, **152**, 37-40, doi: 10.1016/S0020-1693(00)90727-8.

[21] W. L. Armarego, D. D. Perrin, D. R. Perrin, Purification of Laboratory Chemicals, Pergamon Press. London, 1998, p. 260.

[22] S. A. Salunke, L. Kathawate, V. G. Puranik, *J. Mol. Struct.*, 2012, **1022**, 189-196, doi: 10.1016/j.molstruc.2012.05.012.

[23] K. Y. Chu, J. Griffiths, *J. Chem. Soc., Perkin Trans. 1*, 1978, **1**, 1083-1087, doi: 10.1039/P19780001083.

[24] S. Salunke-Gawali, E. Pereira, U. Dar, S. Bhand, *J. Mol. Struct.*, 2017, **1148**, 435-458, doi: 10.1016/j.molstruc.2017.06.130.

[25] U. Dar, S. Bhand, D. N. Lande, S. S. Rao, Y. P. Patil, S. P.

Gejji, M. Nethaji, T. Weyhermüller, S. Salunke-Gawali, *Polyhedron*, 2016, **113**, 61–72, doi: 10.1016/j.poly.2016.04.002.
[26] D. Choudhari, S. Salunke-Gawali, D. Chakravarty, S. R. Shaikh, D. N. Lande, S. P. Gejji, P. K. Rao, S. Satpute, V. G. Puranik, R. Gonnade, 2020, *New J. Chem.,* **17**, 6889-6901, doi: 10.1039/C9NJ04339J.
[27] G. V. Bourrouet, V. M. U. Saldívar, M. Gómez, L. A. O. Frade, *Electrochim. Acta*, 2010, **55**, 9042-9050, doi: 10.1016/j.electacta.2010.08.006.
[28] A. Earnshaw, Introduction to Magnetochemistry, Academic Press, 1968, p. 34.
[29] A. Kunishita, H. Ishimaru, S. Nakashima, T. Ogura, S. Itoh, *J. Am. Chem. Soc.*, 2008, **130**, 4244-4245, doi: 10.1021/ja800443s.
[30] J. Camus, A. Meghea, J. R. Anacona, *Polyhedron*, 1996, **15**, 2953-2958, doi: 10.1016/0277-5387(95)00573-0.
[31] S. Salunke-Gawali, S. Y. Rane, V. G. Puranik, C. Guyard-Duhayon, F.Varret, *Polyhedron*, 2004, **23**, 2541-2547, doi: 10.1016/j.poly.2004.08.022.
[32] T. S. Lobana, R. Sharma, G. Bawa, S. Khanna, *Coord. Chem. Rev.*, 2009, **253**, 977-1055, doi: 10.1016/j.ccr.2008.07.004.

Author information

Umar Ali Dar *is Currently working as Ph.D. (SRF) fellow at Department of Chemistry, National Institute of Technology Srinagar-190006, J&K, India. He has pursued his M.Phil. degree under mentorship of Professor Sunita Salunke-Gawali (2015) and Master's degree in Organic Chemistry (2012) at Savitribai Phule Pune University. He has qualified for National Competitive exams for doctoral fellowships (CSIR-NET/ GATE). The active area of research work for the author is designing and formulation of 1D, 2D and 3D structural motifs of quinone compounds as porous materials.*

Sunita Salunke-Gawali *She received her M.Sc. (1993) in Inorganic Chemistry and Ph.D. (1999) from Pune University. As a professional experience she worked as Post-doctoral Research Associate at Laboratoire de Magnétisme et d'Optique, Versailles France (Prof. F. Varret, 2001-2002), Department of Chemistry, IIT Bombay, India (Prof. C. P. Rao, 2002 and 2004), Universidade do Porto, Portugal, (Prof. Eulália Pereira 2004-2007) and Max-Planck-Institut für Bioanorganische Chemie, Mülheim an der Ruhr, Germany (Dr. Eckhard Bill, 2007- 2008). She joined as Reader in Department of Chemistry, Savitribai Phule Pune University in 2008, where she serves as Professor. Her research interests include coordination and bioorganic Chemistry of naphthoquinone ligands, developing photosensitizer for DSSC, HPLC method development for anticancer drugs and separation of tautomers, chemosensors and metallosurfactants. She is the author of more than 88 articles in international journals.*

Sujit Bhand *is post-doctoral fellow at Centre for Material for Electronic Technology (C-MET) Pune (Dr. Bharat Kale, 2020-till date). He did his Ph.D. at Pune University (2019) with Professor Sunita Salunke as a mentor. After Ph.D. he did his Post-doctoral research with Dr. Nirmalya Ballav in Indian Institute of science Education and research (IISER) Pune (2018-2020). His research interests are DSSC, Naphthoquinone chemistry, coordination polymer for electrocatalyst and electronic devices application, flexible Lithium ion battery.*

Dnyaneshwar R. Shinde *is Professor at Department of Chemistry, of Prof. Ramkrishna More Arts, Commerce and Science college, Akurdi, Pune 411044 since 1998. The college is affiliated to the Savitribai Phule Pune University (SPPU). He did his Ph.D. (2010) at SPPU and also completed minor research project funded by SPPU. His research interests are coordination chemistry, materials chemistry and application of nanomaterials in gas sensors, pollution degradation, organic synthesis and dye sensitized solar cells. He is the author of more than 20 articles in international journals.*

Surekha K. Satpute *is an Assistant Professor at Department of Microbiology, Savitribai Phule Pune University (SPPU) since 2016. She did her Ph.D. (2009) at Pune University. She has worked as Women Scientist under (WOSA-A), {SR/WOS-A/LS-1076/2014(G)}, Department of Science and Technology, Government of India scheme at the Department of Physics, SPPU (2014-2017). Her research areas of interests are biosurfactant/bioemulsifiers, biofilms, nanotechnology, medical microbiology, marine biology, microbial technology. She is an author of more than 37 review and research articles in national and international peer reviewed journals.*

Publisher's Note: Engineered Science Publisher remains neutral with regard to jurisdictional claims in published maps and institutional affiliations.